

# Microstructure of tropospheric aerosol in Siberia as judged from photoelectric particle-counter measurements

M.V. Panchenko and V.V. Pol'kin

*Institute of Atmospheric Optics,  
Siberian Branch of the Russian Academy of Sciences, Tomsk*

Received March 15, 2001

This work is a step in the development of a dynamic regional model of optical characteristics of tropospheric aerosol in Siberia based on data of long-term airborne measurements. The model of aerosol microstructure is based on measurements with a photoelectric particle counter. Interpreting of experimental data uses a representation of the particle size-distribution by a superposition of three lognormal distributions. The model provides for a satisfactorily good reconstruction of optical characteristics of aerosol in the visible spectral region.

## Introduction

The regional dynamic model of optical characteristics of the tropospheric aerosol in Siberia proposed is based on the data of long-term airborne measurements.

The empirical basis for the regional model are the results of analysis of a statistically significant array of experimental data, whose geophysical significance is confirmed by comparison of synoptic features and meteorological parameters with similar data of long-term observations in this region.<sup>1</sup>

The first stage, whose results have been reported in Refs. 1–6, consisted in the development of a model of the vertical profile of the scattering coefficient for radiation at 0.52  $\mu\text{m}$  wavelength. In that model, the reconstruction scheme provides for the possibility of multi-choice accounting for *a priori* information, external seasonal and synoptic features, as well as measured optical and meteorological characteristics.

This plan of model development was dictated by the following considerations. The scattering coefficient sums up the properties of the entire ensemble of submicron particles<sup>7</sup> and their variability under the effect of external geophysical and meteorological factors. It is one of the most sensitive characteristics reacting to practically any change in the size spectrum and complex refractive index of the submicron particles.<sup>8</sup> As a consequence, it is just the scattering coefficient at the wavelengths in the green spectral region that is an input parameter for almost all earlier few-parameter models of the atmospheric near-ground layer.<sup>7,9</sup> This allows other optical characteristics to be estimated along the entire vertical profile with a certain degree of accuracy already at the first stage.

Airborne nephelometric measurements of the coefficients of directed scattering<sup>1</sup> have allowed us to study separately the space and time variability of the dry substance content and condensation activity of submicron aerosol particles. This approach has provided

for more adequate evaluation of the role of geophysical processes of different spatiotemporal scale in the formation of optical state of the regional atmosphere than the use of the data of direct *in situ* observations (see, for example, Refs. 1 and 2).

Photoelectric counter measurements produce the data in a limited range of particle size (in most cases, direct calculations of optical parameters show that if the size spectrum is known only within the counter's sensitivity range, only up to tens percent of the actual value of the scattering coefficient for the wavelengths in the visible spectral region can be reconstructed).

At the same time, it is clear that the size-distribution function transforms in some way with height and, consequently, few-parameter representations obtained for the near-ground layer can be applied only for very rough estimates.

To extend the model capabilities in reconstructing not only the scattering coefficient profile at a single wavelength, but other optical characteristics as well, it seems reasonable to compliment the model with certain representation of the vertical distribution of the main parameters of aerosol particle microstructure as estimated from the data obtained with a photoelectric counter.

It should be emphasized that all airborne measurements of the aerosol microstructure with a photoelectric counter were conducted by the group headed by Prof. B.D. Belan we are grateful to them for the possibility granted of using these data.

## Analysis of data measured with a photoelectric particle counter

To pass to estimation of the distribution parameters, let us analyze the measurement data. Taking into account high correlation between the scattering coefficient and the number density of particles with the radius  $r > 0.2 \mu\text{m}$ , we can assume that the main features of the number density profile

measured with a photoelectric counter must be similar to the features that are allowed for in the model of the vertical profile of the scattering coefficient.<sup>1–6</sup> To refrain from repetition in description of the processes causing variability of the profiles of aerosol characteristics, let us restrict our consideration to brief review of the experimental material.

### Seasonal variability of the particle number density

Consider the seasonal variability of the number density  $N$  ( $r > 0.2 \mu\text{m}$ ) for the Western Siberia in 1986–1988, i.e., using the same data array as that used in developing the model of the scattering coefficient.

Figure 1 shows vertical profiles of  $N$  ( $r > 0.2 \mu\text{m}$ ) in the altitude range from 0 to 5.5 km both for the absolute values of  $N$  ( $\text{l}^{-1}$ ) (Fig. 1a, left) and for the values normalized to the surface number density ( $h = 0$  km) (right). Figure 1b shows the histograms of the number of measurements for different altitudes ( $\Delta h = 100$  m) for all seasons. Variations of the number density  $N$  ( $r > 0.2 \mu\text{m}$ ) in the analyzed altitude range make up more than two orders of magnitude.

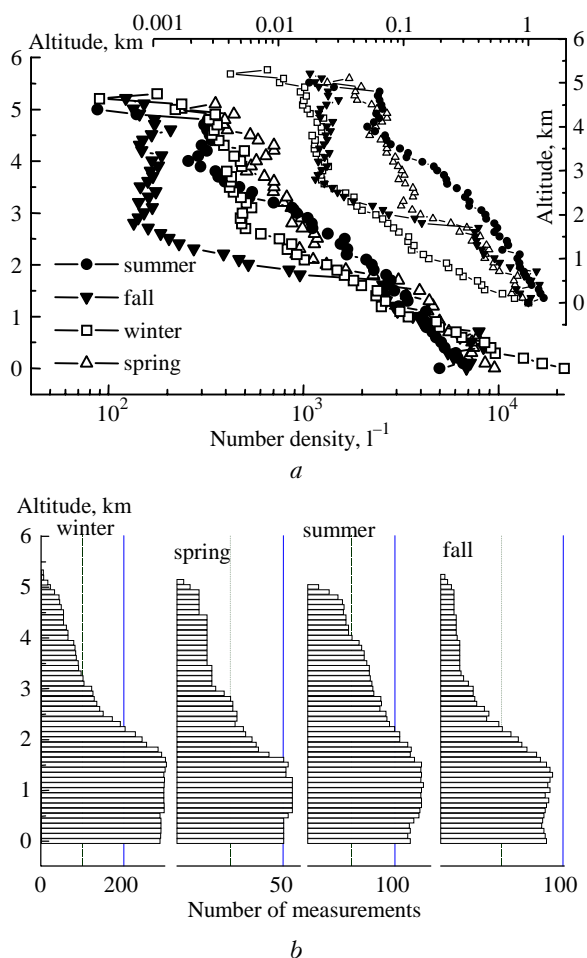


Fig. 1. Seasonal variability of vertical profiles of number density  $N$  ( $r > 0.2 \mu\text{m}$ ).

The vertical stratification  $N(h)$  varies markedly from season to season. Apparently, the shape of the vertical profile is mostly caused by thermal conditions in the atmosphere. Actually, differences in  $N(h)$  stratification are maximum for the most contrasting seasons (winter–summer, see Fig. 1a).

The vertical profiles of  $N(h)$  up to the altitude of 2 km observed in the spring and fall seasons are close to each other being intermediate between the winter and summer profiles. Above 2 km, the atmosphere is overfilled with aerosol in spring because of the effect of distant sources caused by thawing of snow in southwestern regions.<sup>1</sup>

The main regularities in the  $N(h)$  variability can be schematically presented, as in Refs. 10–15, in the form of a three-layer altitude distribution of aerosol in the following altitude ranges:  $0-h_1$  – near-ground layer (immediately adjacent to the surface, characterized by high atmospheric turbidity),  $h_1-h_2$  – boundary layer or layer of active turbulent exchange (mixing layer characterized by more or less constant value of the aerosol number density); above  $h_2$  – free atmosphere (also with roughly constant value of the number density  $N$ ). Between the mixing layer and the free atmosphere, there exists an intermediate zone about 200–400 m thick.

The largest variations of the number density and meteorological parameters are observed in the near-ground layer. The effect of the surface, season, temporal parameters, etc., on the aerosol number density is most pronounced here. In the models from Refs. 10 and 15, a fast drop of the aerosol number density with height was noticed in the near-ground layer. Actually, it is not always the case. As was shown in Ref. 1, the pronounced drop of the aerosol content in the near-ground layer in summer is observed almost always in arctic air masses, whereas in midlatitude air masses it is observed only in the high-pressure zones. In fall this behavior of aerosol shows itself only in arctic air masses.

### Altitude variability of the particle size-distribution

Using the obtained array of data in the altitude range of 0–5 km, we have analyzed the profiles of 12 aerosol fractions with the particle diameter ranging from 0.4 to  $10 \mu\text{m}$  (more than 5000 spectra for Western Siberia dated to 1986–1988) with the altitude step of 100 m. Before analysis of the size spectra, let us note some needed methodic aspects to be kept in mind while operating photoelectric particle counters.

The boundaries of size spectra measured with a counter, as was shown in Ref. 16, depend on the refractive index of the particulate matter. The larger is the difference between the refractive index of actual particles from that of the particles, against which the counter was calibrated (in our case, the calibration value  $n = 1.6$ ), the larger is the correction needed to determine the “true” size.<sup>16</sup>

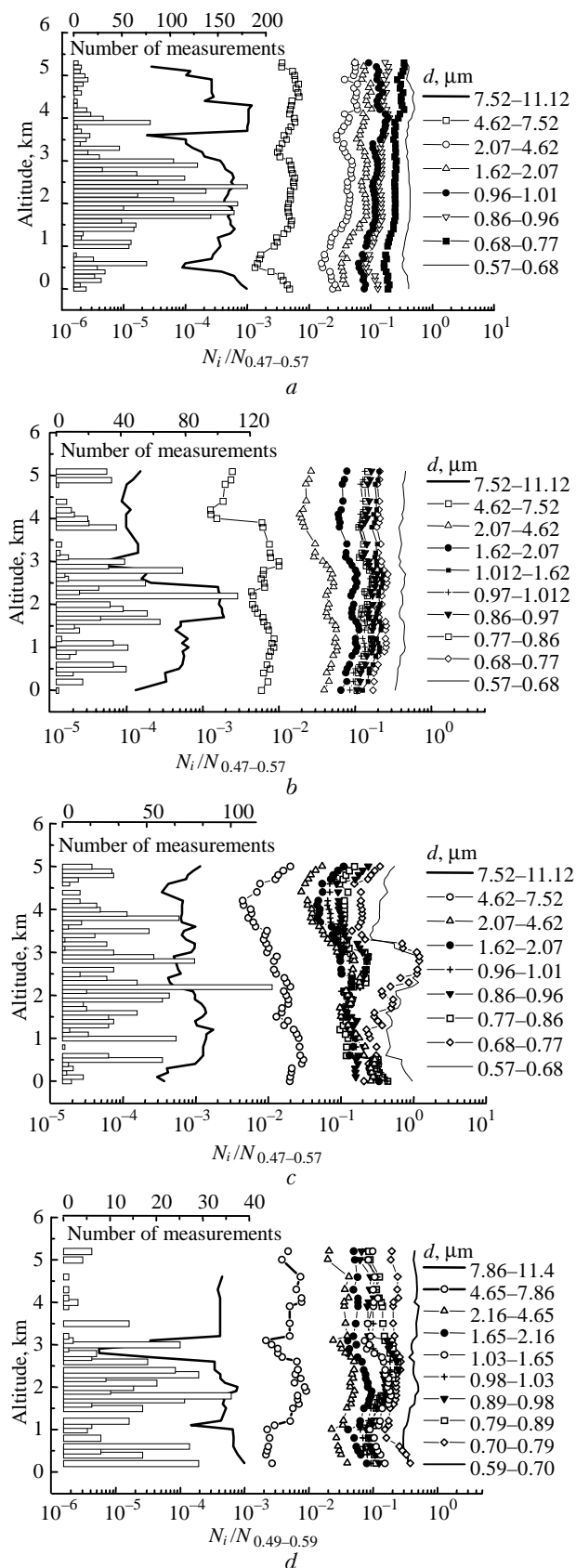


**Fig. 2.** Normalized number density of different fractions of aerosol particles: winter (a), spring (b), summer (c), and fall (d) of 1986–1988.

It is clear that the refractive index of aerosol particles strongly depends on variations of the relative air humidity, which, consequently, should be taken into account in processing the measurement data. Apparently, it is impossible to correct rigorously every measured spectrum, because neither refractive index nor the condensation activity of aerosol particles in a specific atmospheric situation is known with the accuracy needed. Therefore, we used the following procedure in the data processing. The season-mean value of the relative air humidity (for every altitude range) was calculated. According to Ivlev's model,<sup>17,18</sup> the refractive index was specified for the given range of humidity values. Then, using the approximation from Eq. 19, the "actual" boundaries were calculated for 12 operating ranges of the counter.

For four seasons of 1986–1988,<sup>6</sup> Fig. 2 shows vertical number density profiles for different size fractions of aerosol particles. The profiles are normalized to the number density of particles of the first range of the photoelectric counter. The curves are smoothed by the method of moving average over three points.

The horizontal bars show the number of measurements at every altitude. We can see that the number of experimental data above the mixing layer is low for each season; consequently, in this range we cannot expect that the model gives a good altitude resolution.

It is seen from Fig. 2 that, in the first approximation, the relative contribution coming from particles with the size falling in the counter's measurement range to the size spectrum only slightly varies with height. Only in summer the high content of particles with the diameter of 0.6–0.8  $\mu\text{m}$  is well pronounced at the altitudes adjacent to the upper boundary of the mixing layer (from 1.5 to 3 km).

### Approximation of the distribution function

In the overwhelming majority of experimental measurements, the particle size-distribution function is approximated by a lognormal distribution or superposition of several lognormal distributions:

$$\Delta V / \Delta r = \frac{1}{\sqrt{2\pi}} \sum_{i=1}^n \frac{V_i}{\ln \sigma_i r} \exp \left( -\frac{\ln^2(r/r_i)}{2 \ln^2 \sigma_i} \right) \quad (1)$$

where  $r$  is the particle radius,  $\sigma_i$  is the variance of the distribution of the  $i$ th mode;  $r_i$  and  $V_i$  are the modal value of the radius and the fill factor of the  $i$ th mode, respectively.

In current models, the microstructure of tropospheric aerosol is usually presented by three principal fractions. Following Refs. 20 and 21, we call them the micron, submicron, and coarse fractions (some other papers use other names for these three fractions;

see, e.g., Ref. 22). It is clear that for a detailed description of optical characteristics in a wide spectral region, all parameters of each fraction should be known well enough. In formation of optical properties of atmospheric aerosol in the visible spectral region, the main role belongs to the submicron particles, whereas particles of other two fractions contribute less significantly. Their manifestations are marked only in some optical parameters; for example, coarse particles manifest themselves mostly in the region of aureole scattering angles and in their spectrally neutral contribution to the extinction coefficient.

At the same time, we cannot completely neglect the contribution of the micron and coarse particles when estimating any optical characteristic in the visible region. Moreover, even at numerical simulation of the aerosol microstructure, these fractions can hardly be separated rigorously. Therefore, when reconstructing microphysical characteristics from the data of optical measurements in the visible spectral region, the particle size-distribution function is most often described as a wide lognormal distribution of submicron particles formally covering some portions of the micron and coarse fractions.

Photoelectric counters of aerosol particles, because of their technical and methodic capabilities, give information on particles, whose size spectrum only partially covers the drop-down branch of the distribution function of the submicron fraction, and quite well reflect the aerosol microstructure in the range of several microns. The above-said suggests the following principal conclusions.

1. There exists a possibility of judging on the aerosol microstructure from experimental data obtained with a photoelectric counter; these data will be useful for estimating optical characteristics.

2. Formal extrapolation to the ranges lying beyond the counter sensitivity should be based on some *a priori* knowledge of the shape of the distribution function, and parameters should be chosen by comparison with the corresponding data of direct measurements of optical characteristics.

Thus, when approximating the experimental data, we assume that the following conditions are met: (a) The shape of the function and variability of its basic parameters do not contradict general concepts on the properties of atmospheric aerosol; (b) When estimating the likelihood of the reconstructed parameters of the particle size-distribution function, the main criterion is the agreement of the measured spectrum of the scattering coefficients and angular behavior of the degree of linear polarization of scattered radiation with those calculated by the Mie theory within the experimental accuracy.

It is clear that fulfillment of only two not rigorously defined conditions leaves marked arbitrariness in the description of particle size spectrum and a considerable number of its possible features prove to be ignored. At the same time, the requirement of a

small number of parameters in the model itself apparently implies simplification of the description of microstructure parameters. Since the main purpose of our work is to extend capabilities of the model of vertical profile of the scattering coefficient in estimating optical characteristics (at least, not at only single wavelength) based on microphysical concepts, there is a good reason to think that the conditions formulated above are quite adequate to the problem to be solved.

Actually, all few-parameter models use wide lognormal particle size distributions. In its turn, it is known that for wide lognormal distributions of submicron particles in the visible spectral region (the authors are primordially skeptic about the possibility of reconstructing the aerosol optics in the IR and UV spectral regions with the use of this approach) the most sensitive characteristics are scattering coefficient, its wavelength dependence, and the angular distribution of the degree of linear polarization of scattered radiation. At a constant refractive index, these characteristics almost invariantly react to variations of the modal radius or the width of the distribution (it should be emphasized that the latter concerns only the wide distributions). All other optical parameters vary within more narrow limits. Consequently, if we succeed in choosing such parameters of the size-distribution function that provide an agreement with the experimentally observed characteristics mentioned above, we may have grounds to believe that the problem is solved at this stage. Apparently, the microphysical pattern obtained at this approach is of little use for some in-depth conclusions on the processes of transformation of the size-distribution function with height, but it is useful for estimation of optical characteristics.

Taking into account the fact that the microstructure characteristics most important for description of the scattered radiation are the geometrical cross section of a particle and the scattering efficiency factor (which is directly proportional to the particle size in the range of small values of the Mie parameter<sup>22</sup>), it is worth approximating volume distributions rather than linear ones.

The typical shape of the size distribution function obtained in such a way is shown in Fig. 3.

Here squares denote the experimental values of  $\Delta V(r)/\Delta r$ , and curves correspond to the approximation (rendering in Fig. 3 shows the regions of increasing uncertainty in function setting – worsening of the quality of the extrapolation).

We can see that this type of the microstructure can be well described by a combination of three lognormal distributions. Since the positions of the three fractions on the size scale (see Fig. 3) not that well correspond to canonical representation of the three-fraction composition of aerosol,<sup>20,21</sup> let us denote them as *A*, *B*, and *C*.

In this case, the fraction *A* covers not only submicron, but also a portion of the micron particles.

Obviously, extrapolating the size-distribution function sufficiently far from experimental points, we introduce some arbitrariness. The use of such data can be justified by having in mind the following arguments.

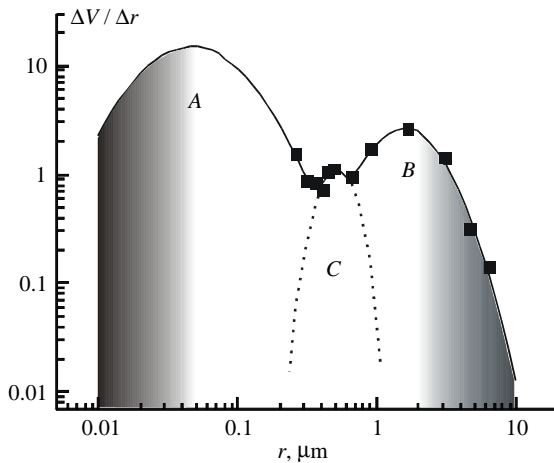


Fig. 3.

First, from the very beginning we planned to deal with the optically most active particles having wide size-distributions.

Second, particles with the size of several hundredths micron are interpreted as Rayleigh ones in the visible spectral region, and an important characteristic in formation of optical properties is the amount of particles, rather than the form of their size distribution function.

Now it is appropriate to present some ideas on using wide lognormal distributions covering the submicron and micron ranges of particle sizes. Actually, a wide lognormal size distribution well describes only some mean observed aerosol microstructure, if averaging is performed over a large array of various atmospheric situations. For static models it is quite applicable for estimation of optical characteristics (see, for example, Ref. 7). At the same time, physics of the processes proceeding in the atmosphere far from local sources of aerosol and aerosol-generating substances does not allow, as a rule, long coexistence of a large amount of submicron and micron particles.

In the case that the concentration of submicron particles in air is high enough, the main sink of vapor of aerosol-generating substances, clusters, and micron particles themselves goes into the developed surface of the submicron aerosol.<sup>20,21,23</sup> On the contrary, in the absence of "sufficient" amount of submicron aerosol, vapors of aerosol-generating compounds can pass the whole path from cluster to a particle and make up a representative micron fraction.

Hereof, a somewhat paradoxical conclusion follows that in the actual "background" atmosphere, the situation with microphysical characteristics corresponding to the common model representation at the particle size ranging in the transient zone between the micron and submicron fractions is unlikely. Or, in

other words, for atmospheric situations with a developed submicron fraction, the microphysical model should include the faster drop of the number density of the smallest particles than that allowed by a wide lognormal distribution.

These conclusions are confirmed not only by direct measurements of the microstructure<sup>23,24</sup> (which, unfortunately, are still insufficient to correctly describe the shape of the function in this size range), but also by optical manifestations. In particular, when calculations are performed within the framework of wide lognormal distributions, it is impossible to reconstruct the experimentally observed slowing-down growth of spectral extinction coefficients at transition from the wavelength of 0.5 μm to the shorter-wave spectral region (see, for example, Ref. 9).

The defect of representation of the microstructure in the form of the fraction *A* is hardly noticeable when describing power parameters of the scattered radiation in the region of wavelengths longer than 0.5 μm. It may manifest itself when evaluating polarization of the scattered radiation, but its effect can be excluded when describing static situations by the proper choice of the modal radius and the width of the distribution.

The situation is quite different, if the microphysical model implies description of the dynamics of optical characteristics, for example, under the effect of air humidity, whose increase can cause the growth of small particles into the optically active ones. In this case, all errors of approximation of the distribution function in this size range can seriously distort the pattern of transformation of angular polarization characteristics. To decrease the effect of these errors, we have developed a number of methodic approaches, which will be described below.

Let us now consider in a more detail the fraction of the largest particles – fraction *B*. The particles of the size range from several tenths to 1–2 μm are most reliably recorded by a photoelectric counter (keeping in mind the need to take into account the refractive index of particles) and well approximated by the approximating curve. The situation beyond the counter measurement range, as well as the case of finest particles, calls for additional comments. Poor knowledge of the behavior of the size-distribution function of the coarse fraction introduces certain distortions in the description of aureole scattering angles and does not allow the model applicability to be extended to the IR spectral region.

In the angular dependence of the degree of linear polarization, coarse particles are most pronounced in the rainbow zone. Actually, the calculated and experimental polarization characteristics in this range of angles often differ markedly. This happens mostly because the phenomenon of rainbow is observed only with the ideally spherical particles (this is fixed by model calculation), whereas actual aerosol particles in this size range hardly have a strictly spherical shape. Even a minor deviation from the spherical shape

obscures the manifestation of large particles in polarization in rainbow zones, and therefore insufficient knowledge of the shape of the distribution function in the range of coarse particles, because of their nonsphericity, has a weak effect on formation of the angular structure of the degree of linear polarization of the scattered radiation in the visible spectral region.

As to the fraction  $C$  (see Fig. 3), note that the nonmonotonic character of the distribution function in this size range can be smoothed without large prejudice to the accuracy of reconstruction of optical characteristics, and the microstructure can be described only by the fractions  $A$  and  $B$ . But, on the one hand, retention of this rather narrow fraction  $C$  in description of the entire spectrum formally decreases considerably the error of approximation in the size range directly measurable by a particle counter. On the other hand, this fraction is well marked in most atmospheric realizations. As an example, Fig. 4 shows the size distribution function from the data obtained in the atmospheric near-ground layer at the automated aerosol station of the Laboratory of Aerosol Optics (<http://aerosol1.iao.ru/>). We can see that during a day this peculiarity is well pronounced for every specific measurement cycle even at 24-hour averaging. There is a reason to suppose that this narrow fraction is the most long-lived one in the atmosphere and in certain situations it can have a decisive significance in

formation of the optical state of the entire atmospheric column.<sup>25,26</sup>

Figure 5 shows the averaged experimental data and the corresponding approximating curves for different seasons and certain altitudes. The experimental data were approximated in different ways. The values of  $\Delta V(r)/\Delta r$  normalized to the measured total number density of particles were approximated. This normalization was performed for each realization, and then the mean curve for every altitude range was determined. Such an approach makes the distribution function free from the influence of the concentration effect and allows us to reveal the main features in the behavior of  $\Delta V/\Delta r$ . In this case,  $\Delta V/\Delta r$  of individual measurements is included in the statistics for average  $\Delta V/\Delta r$  with the same weighting factor independent of the total number density of each separate  $i$ th measurement.

The experimental data were averaged over altitudes in such a way to consider most thoroughly the main parts of the vertical profile within the three-layer representation and their seasonal variability. Inside these parts, the averaging ranges were chosen so that each of them included roughly the same and representative number of spectra.

Analysis has shown that within the acceptable errors, regardless of season, for the fraction  $A$  we can neglect the variability of the distribution width and the value of  $\ln\sigma_A$  for these particles can be taken equal to 0.8.

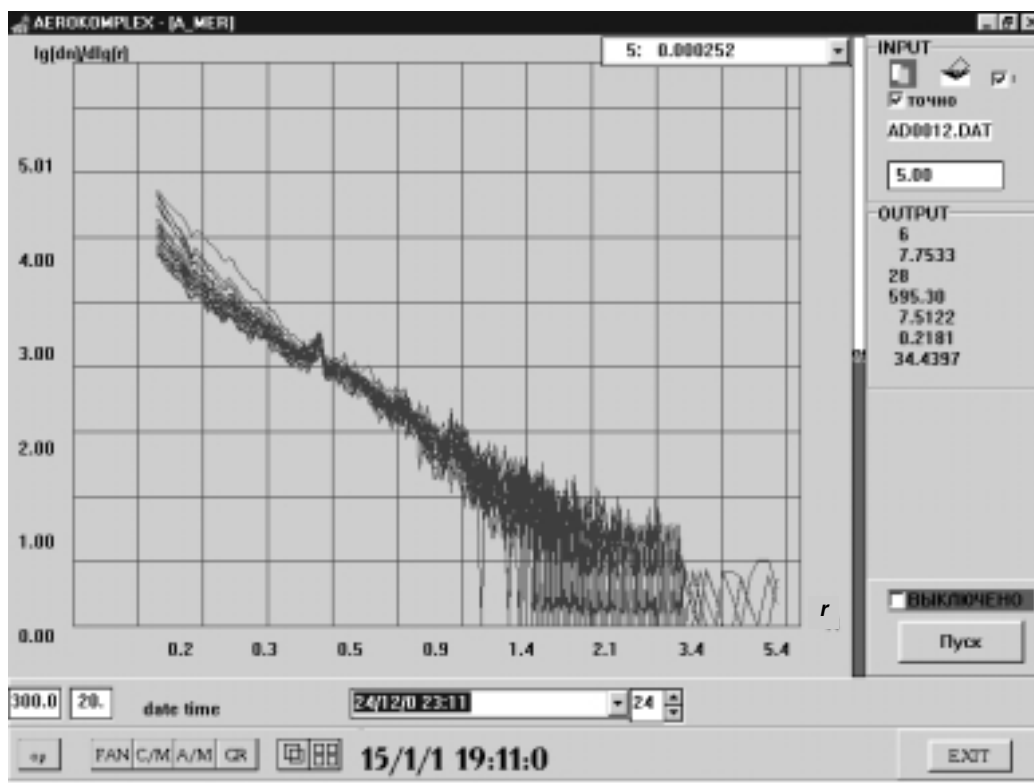


Fig. 4.

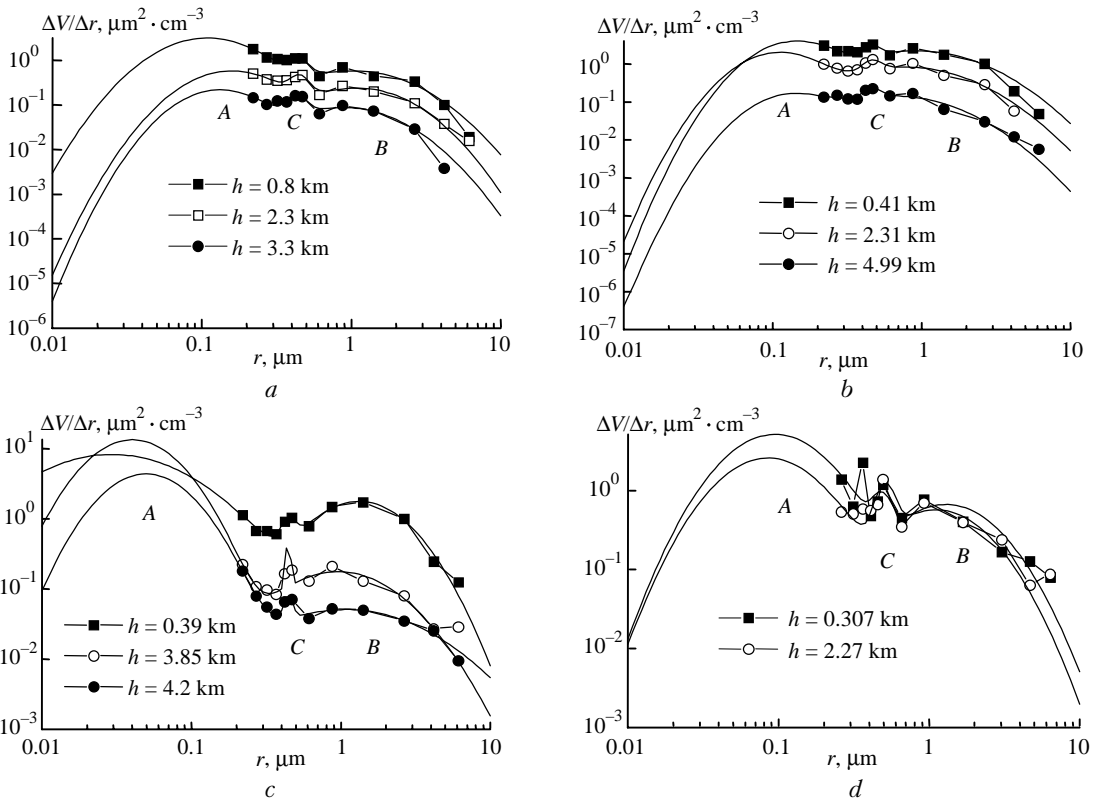


Fig. 5. Most typical experimental data and theoretical approximation curves corresponding to these data: winter (a), spring (b), summer (c), and fall (d) of 1986–1988.

Table. Microphysical model of vertical profile

Parameters of the function	Fraction		
	A	B	C
<b>Winter</b>			
$\ln \sigma$	0.8	0.75	0 – 0.243 km    0.148 – 0.32h 0.243 – 5 km    0.07
$r, \mu\text{m}$	0.093	0 – 0.243 km    3.63 – 7.67h 0.243 – 5 km    1.77 + 0.0079h	0.5
$V \cdot 10^{12} / \sqrt{2\pi}$	0 – 0.243 km $N_w(0.79 + 0.23h)$ 0.243 – 2.4 km $N_w(0.86 - 0.086h)$ 2.4 – 5.3 km $N_w \cdot 0.66$	$N_w(0.94 - 2.44h)$ $N_w(0.33 + 0.12h)$ $N_w \cdot 0.62$	$N_w(0.078 - 0.22h)$ $N_w(0.026 - 0.00067h)$ $N_w \cdot 0.042$
<b>Spring</b>			
$\ln \sigma$	0.8	0.8	0.03
$r, \mu\text{m}$	0 – 1 km    0.032 – 0.0013h 1 – 5 km    0.026 + 0.0057h	0 – 1.39 km    1.4 + 0.196h 1.39 – 5 km    1.18 + 2.4 × × exp(-h/0.88)	0.456
$V \cdot 10^{12} / \sqrt{2\pi}$	0 – 1.39 km $N_{spr}(4.705 - 0.184h)$ 1.39 – 5 km $N_{spr}[0.72 +$ + 14.7 · exp(-h/1.012)]	$N_{spr}(0.646 + 0.316h)$ $N_{spr}(1.22 - 0.156h)$	$N_{spr}(0.305 + 0.0173h)$
<b>Summer</b>			
$\ln \sigma$	0.8	0.65	0 – 0.275 km    0.053 – 0.082h 0.275 – 5 km    0.03
$r, \mu\text{m}$	0 – 0.275 km    0.099 – 0.077h 0.275 – 5 km    0.078	2.078 – 0.97h 1.81 – 0.013h	0.463
$V \cdot 10^{12} / \sqrt{2\pi}$	0 – 0.275 km $N_{sum}(0.69+0.92h)$ 0.275 – 5 km $N_{sum}(0.94+0.01h)$	$N_{sum}(0.51 - 2.06h)$ $N_{sum}(1.09 - 0.07h)$	$N_{sum}(0.056 - 0.085h)$ $N_{sum}(0.032 - 0.0009h)$
<b>Fall</b>			
$\ln \sigma$	0.8	0.68	0.05
$r, \mu\text{m}$	0.051	0 – 2 km    1.52+0.18h 2 – 5 km    1.68+3.45 exp(-h/0.62)	0.5
$V \cdot 10^{12} / \sqrt{2\pi}$	$N_f(1.63 - 0.041h)$	$N_f(0.87 - 0.024h)$	$N_f \cdot 0.03$

Note.  $N_w, N_{spr}, N_{sum},$  and  $N_f(h)$ , in  $\text{cm}^{-3}$ , are the absolute number densities measured with a photoelectric counter for the mean vertical profiles of the number density in winter, spring, summer, and fall, respectively;  $h$  is the altitude, in km.

To describe the behavior of the variance of  $\ln\sigma_{B,C}$  for the fractions  $B$  and  $C$  in different seasons and altitude ranges, we had to make the linear approximation.

Using the preset mean values of the variance for the fractions (in different seasons and altitude ranges), we have determined the values of the modal radius. Having estimated the variance and the positions of the modes for the particle fractions, we have calculated the fill factors for each fraction  $V_i$ . The obtained estimates of the altitude dependence  $V_i(h)$  were approximated by linear dependences on the altitude  $h$ . The results of this approximation for different seasons, as well as the values of the variance and the modal radius for the fractions are given in the Table. To reconstruct the particle size distribution function for a specific atmospheric situation, in which the vertical profile of the particle number density is measured with an aerosol counter, it is needed to calculate  $V_i(h)$  according to the Table by substituting the specific values of  $N(h)$ .

Obviously, the data from the Table represent only the mean pattern of the microphysical model of the vertical profile that corresponds to the mean values of the particle number density and the relative humidity of air for each season. If the dynamics of number density variation for specific situations can be introduced into the model by simple re-normalization of  $N$ , then the allowance for the relative humidity calls for separate consideration.

### Transformation of the size spectrum under the effect of air humidity

Against the background of the whole set of geographic, synoptic, and meteorological factors affecting the variability of the optical state of the atmosphere (and, consequently, the size spectrum of aerosol), the process of condensation transformation is prominent.<sup>10,27–29</sup> The growth of the relative humidity of air is usually associated with the growth of aerosol particles adsorbing moisture in some or other way<sup>18,30</sup> and, as a consequence, with the change of the total refractive index of an aerosol particle. First such investigations performed by Junge<sup>31,32</sup> have led to the theory of mixed nuclei (aerosol particles consist of a conglomerate of soluble and insoluble substances with different chemical properties).

Based on the data on the dependence of the mass of aerosol particles on humidity, Hanel<sup>30</sup> has developed a model of the microstructure of humid continental aerosol on the assumption that the fraction of water-soluble substances in aerosol particles of any size is constant. Qualitatively, the condensation transformation in Hanel's and Junge models of the microstructure of continental aerosol is the same, because both models presume that the fraction of water-soluble substances is independent of the size of dry particles.

Meszaros<sup>27,29</sup> has demonstrated this assumption to be inconsistent.

In Laktionov's semi-empiric theory of equilibrium condensation growth of aerosol particles,<sup>28</sup> the equilibrium radius of a particle  $r_{RH}$  at the relative air humidity  $RH$  is related to the radius of the dry particle  $r_0$  as follows:

$$r_{RH} = r_0 [1 - BE_v / (\ln RH)]^{1/3}, \quad (2)$$

where  $B = 1.13 - 0.422RH$  for the continental type of aerosol.<sup>28</sup>

Having in mind this idea for the development of the model of atmospheric aerosol microstructure, which would allow for variation of the particle size in response to variation of the relative humidity  $RH$ , we need to know the dependence of the volume fraction of water-soluble substances in aerosol particles on their size  $E_v(r)$ . The parameter  $E_v$  is defined as the ratio of the volume of water-soluble particles to the volume of all dry particles. The sought dependence was determined by different methods for different types of aerosol (rural, urban, oceanic, continental, etc.).<sup>27,29</sup>

The attempts to make agree the variability of optical characteristics observed in our experiments (first of the scattering coefficient and the degree of polarization of the radiation scattered at the angle of  $90^\circ$ ) and the variability of optical characteristics calculated theoretically with the use of the data from Refs. 27–29 and 31 on the dependence of the fraction of soluble substances on the particle radius failed.

Figure 6 shows the dependences of the degree of linear polarization  $P$  (Fig. 6a) (these dependences follow from the empiric model of coastal atmospheric haze<sup>9</sup>) and the typical dependences of  $P$  for the radiation scattered at the angle of  $90^\circ$  (Fig. 6b) obtained in our experiments at artificial moistening.<sup>33</sup>

Using  $E_v(r)$  in the form corresponding to the literature data<sup>27–29,31</sup> at the increase of the relative humidity we succeeded only in providing for the likely growth of the scattering coefficient, while the degree of polarization either remained constant or increased, and this behavior contradicts the experimental data.

Just at this stage the defects of approximation of the particle size distribution function in the area of small particles manifested themselves. It turned out that if a wide lognormal distribution of particles of the fraction  $A$  is used, the rate of growth of the scattering coefficient and the corresponding drop of the degree of polarization can be agreed with the experimental data only at formally decreasing condensation activity of the finest aerosol particles with the size smaller than  $0.1 \mu\text{m}$ . The form of the distribution in this range of sizes and their connection with external factors are still poorly studied (and the condensation activity of such particles is to be studied thoroughly in the experiments). Therefore, to take advantage of a simple representation in the form of a unimodal wide fraction  $A$ , we decided to use the function  $E_v(r)$ , which describes the dependence of the volume fraction of water-soluble substances as a filter. On the one hand, this filter represents the effect of humidity on the optically active particles according to the well-known



experimental data. On the other hand, it decreases the effect of approximation errors and uncertainties in the experimental data on condensation activity of the finest particles.

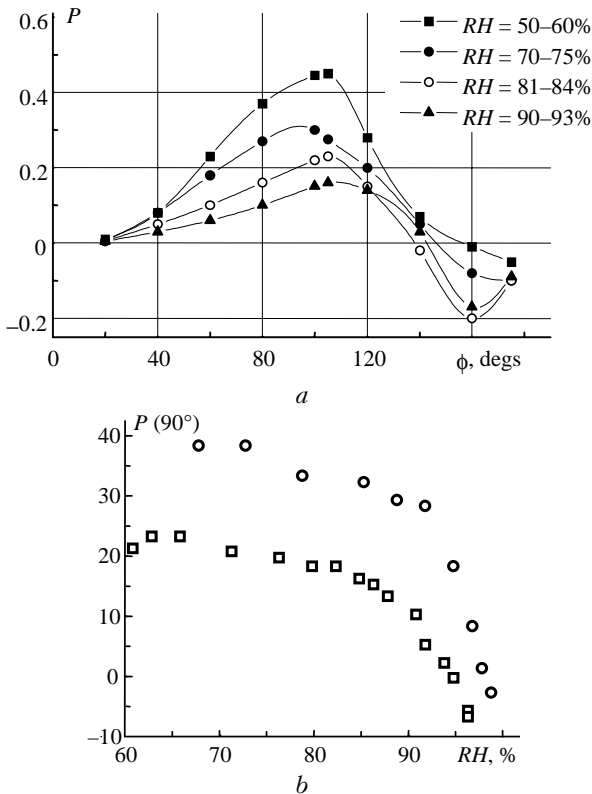


**Fig. 6.** Most typical dependences: degree of linear polarization  $P$  for the empiric model of coastal atmospheric haze<sup>9</sup> (a) and degree of linear polarization  $P$  for radiation scattered at the angle of  $90^\circ$  for experiments with artificial moistening<sup>33</sup> (b).

To describe the dependence  $E_v(r)$  used as a filter, it was proposed to use the unimodal lognormal distribution in the following form:

$$E_v = y_0 + A \exp\left(-0.5 \left[\frac{\ln(r/x_c)}{\omega\omega}\right]^2\right) \quad (3)$$

Then the parameters of this function were chosen from calculations by the Mie theory and comparison with the experimental data<sup>34</sup>:  $y_0 = 0$ ,  $A = 0.4$ ,  $x_c = 0.32 \mu\text{m}$ ;  $\omega\omega = 0.6$ .

To calculate the optical characteristics by the Mie theory, the real part of the complex refractive index was estimated by Hanel's equation<sup>18,30</sup>:

$$n_{RH} = 1.33 + 0.17(r_0/r_{RH})^3. \quad (4)$$

The imaginary part of the complex refractive index was taken as for aerosols of the condensation origin in Ivlev's in Krekov's models.<sup>17</sup> The aerosol microstructure was preset according to the proposed model, and the major computer experiment was conducted for the following parameters (Western Siberia, summer, mean altitude of 0.08 km):

$$V_A = 0.75 \cdot 5.775, V_B = 0.814 \cdot 5.775, V_C = 0.003 \cdot 5.775, \\ \ln\sigma_A = 0.8, \ln\sigma_B = 0.65, \ln\sigma_C = 0.22, \\ r_A = 0.093 \mu\text{m}, r_B = 2.0 \mu\text{m}, r_C = 0.61 \mu\text{m}.$$

For the relative humidity  $RH = 70, 80, \text{ and } 90\%$ , particle radii were calculated by Eq. (2) assuming the total number density of particles unchanged. For a comparison, Fig. 7 shows typical experimental dependences  $E_v(r)$  (Refs. 27–29 and 35).

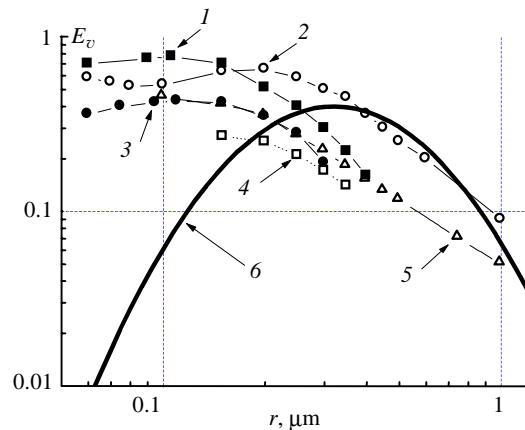


**Fig. 7.** Most typical experimental dependences  $E_v(r)$ : urban aerosol<sup>28</sup> (1), rural aerosol, Hungary<sup>27</sup> (2), winter aerosol, Toronto, Canada<sup>35</sup> (3), summer aerosol, European territory of Russia<sup>29</sup> (4), measurements nearby Zvenigorod<sup>28</sup> (5), dependence proposed by us<sup>34</sup> (6).

We can see that differences are significant only in the range of finest particles.

Since now there is no sufficient experimental information on the distribution function of micron particles and its transformation in the vertical profile for different seasons, the conclusion on the weak condensation activity of these particles should not be drawn based on our computer experiments. At the same time, it should be noted that the experimental data on the effect of humidity on these particles are not numerous, and the role of micron particles in condensation processes is still a question to be addressed. That is why we propose to apprehend the obtained form of the function  $E_v(r)$  as some formal trick, which provides for agreement between the calculated and experimental results when reconstructing optical characteristics using the proposed model of the aerosol microstructure.

Figure 8 shows the distribution functions for the “dried” and moistened aerosol ( $RH = 70, 80, 90\%$ ). These functions were used for calculation of optical characteristics. Figure 9 shows the calculated and experimental data for the angular dependence of the degree of polarization for the radiation at the wavelength  $\lambda = 0.56 \mu\text{m}$  at different values of the relative humidity  $RH$ , and Fig. 10 shows the calculated and experimental data on the spectral behavior of the aerosol scattering coefficient  $\beta_{\text{calc}}$  normalized to

the value of  $\beta_{dry}$  of dry aerosol at  $\lambda = 0.56 \mu\text{m}$  for different  $RH$ .

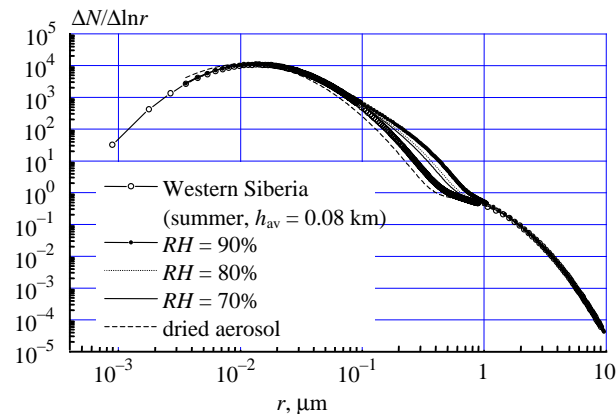


Fig. 8. Distribution functions for dried and moistened aerosol that were used for calculation of optical characteristics.

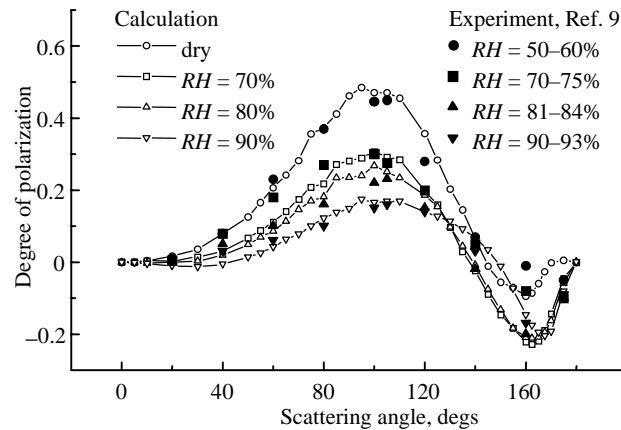


Fig. 9. Calculated and experimental data for angular dependence of the degree of polarization for radiation at  $\lambda = 0.56 \mu\text{m}$  at different relative humidity of air  $RH$ .

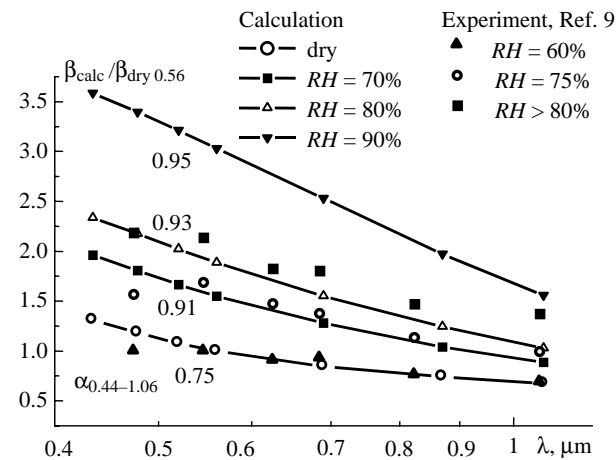


Fig. 10. Calculated and experimental data on the spectral behavior of aerosol scattering coefficient  $\beta_{calc}$  normalized to  $\beta_{dry}$  of dry aerosol at  $\lambda = 0.56 \mu\text{m}$  for different relative humidity of air  $RH$ .

In Fig. 10, the value of the Angstrom exponent  $\alpha$  is given for each spectral curve. We can see a good agreement between the calculated and experimental data in the visible spectral region (up to  $0.7 \mu\text{m}$ ). This allows us to recommend the obtained representation of the aerosol microstructure to be used as a unit of the model of vertical profile providing for estimation of optical characteristics.

### Conclusion

It is worth noting that the proposed microphysical model is based on the representation of particle size-distribution function reconstructed from measurements with a photoelectric particle counter. With this level of our knowledge, this model can be applied to estimating optical characteristics in the visible spectral region. The model allows using the results of direct measurements of particle number density and relative humidity of air. The model can be improved, if reliable experiment information of the annual behavior of the condensation activity of aerosol will be obtained or our knowledge of micron particles will be extended. We plan to discuss the way and methods of model expansion to a wider spectral region in our following papers devoted to the model of optical characteristics.

### References

1. M.V. Panchenko, S.A. Terpigova, A.G. Tumakov, B.D. Belan, and T.M. Rasskazchikova, *Atmos. Oceanic Opt.* **7**, No. 8, 546–551 (1994).
2. M.V. Panchenko and S.A. Terpigova, *Atmos. Oceanic Opt.* **7**, No. 8, 552–557 (1994).
3. M.V. Panchenko and S.A. Terpigova, *Atmos. Oceanic Opt.* **8**, No. 12, 977–980 (1995).
4. M.V. Panchenko and S.A. Terpigova, *Atmos. Oceanic Opt.* **9**, No. 6, 464–468 (1996).
5. M.V. Panchenko and S.A. Terpigova, *Atmos. Oceanic Opt.* **9**, No. 12, 989–996 (1996).
6. M.V. Panchenko, S.A. Terpigova, and V.V. Pol'kin, *Atmos. Oceanic Opt.* **11**, No. 6, 532–539 (1998).
7. G.V. Rozenberg, G.I. Gorchakov, Yu.S. Georgievskii, and Yu.S. Lyubovtseva, in: *Atmospheric Physics and Problems of Climate* (Nauka, Moscow, 1980), pp. 216–257.
8. V.S. Kozlov and V.Ya. Fadeev, "Tables of optical characteristics of light scattering by fine aerosol with lognormal size distribution," Preprint No. 31, Institute of Atmospheric Optics, Tomsk (1981), 65 pp.
9. M.V. Kabanov, M.V. Panchenko, Yu.A. Pkhalagov V.V. Veretennikov, V.N. Uzhegov, and V.Ya. Fadeev, *Optical Properties of Coastal Atmospheric Haze* (Nauka, Novosibirsk, 1988), 201 pp.
10. K.Ya. Kondrat'ev, N.I. Moskalenko, and D.V. Pozdnyakov, *Atmospheric Aerosol* (Gidrometeoizdat, Leningrad, 1983), 224 pp.
11. V.E. Zuev and G.M. Krekov, *Optical Models of the Atmosphere* (Gidrometeoizdat, Leningrad, 1986), 256 pp.
12. K.Ya. Kondrat'ev and D.V. Pozdnyakov, *Aerosol Models of the Atmosphere* (Nauka, Leningrad, 1981), 104 pp.
13. Yu.P. Dyabin, M.V. Tantashev, V.D. Marusyak, and S.O. Mirumyants, *Izv. Akad. Nauk SSSR, Ser. Fiz. Atmos. Okeana* **13**, No. 11, 1205–1211 (1977).

14. K.Ya. Kondrat'ev, N.I. Moskalenko, and V.F. Terzi, Dokl. Akad. Nauk SSSR **259**, No. 1, 814–817 (1981).
15. G.P. Faraponova, Izv. Akad. Nauk SSSR, Ser. Fiz. Atmos. Okeana **1**, No. 6, 605–614 (1965).
16. V.S. Kozlov, V.V. Pol'kin, and V.Ya. Fadeev, Izv. Akad. Nauk SSSR, Ser. Fiz. Atmos. Okeana **18**, No. 4, 428–431 (1982).
17. L.S. Ivlev, *Chemical Composition and Structure of Atmospheric Aerosols* (Leningrad State University Publishing House, Leningrad, 1983), 280 pp.
18. G.M. Krekov and R.F. Rakhimov, *Optical Lidar Model of Continental Aerosol* (Nauka, Novosibirsk, 1982), 198 pp.
19. V.S. Kozlov, M.V. Panchenko, V.V. Pol'kin, and Yu.A. Pkhalagov, Izv. Akad. Nauk SSSR, Ser. Fiz. Atmos. Okeana **23**, No. 3, 286–292 (1987).
20. G.V. Rozenberg, Izv. Akad. Nauk SSSR, Ser. Fiz. Atmos. Okeana **19**, No. 1, 21–35 (1983).
21. G.V. Rozenberg, Izv. Akad. Nauk SSSR, Ser. Fiz. Atmos. Okeana **19**, No. 3, 241–254 (1983).
22. M.V. Kabanov and M.V. Panchenko, *Scattering of Optical Waves by Disperse Media*. Part III. *Atmospheric Aerosol* (Tomsk Affiliate SB RAS, Tomsk, 1984), 189 pp.
23. A.S. Kozlov, A.N. Ankilov, A.M. Baklanov, A.L. Vlasenko, S.I. Eremenko, S.B. Malyshkin, and S.E. Pashchenko, Atmos. Oceanic Opt. **12**, No. 12, 1046–1052 (1999).
24. M.Yu. Arshinov and B.D. Belan, Atmos. Oceanic Opt. **13**, No. 11, 909–916 (2000).
25. S.M. Sakerin, R.F. Rakhimov, E.V. Makienko, and D.M. Kabanov, Atmos. Oceanic Opt. **13**, No. 9, 754–758 (2000).
26. S.M. Sakerin, R.F. Rakhimov, E.V. Makienko, and D.M. Kabanov, Atmos. Oceanic Opt. **13**, No. 9, 759–765 (2000).
27. Meszaros, Atmos. Environ. **12**, No. 12, 2425–2428 (1978).
28. A.G. Laktionov, *Equilibrium Heterogeneous Condensation* (Gidrometeoizdat, Leningrad, 1988), 160 pp.
29. A.G. Laktionov, Izv. Akad. Nauk SSSR, Ser. Fiz. Atmos. Okeana **8**, No. 4, 389–395 (1972).
30. G. Hanel, Adv. in Geophys. **19**, 74–183 (1976).
31. C.E. Junge, *Air Chemistry and Radioactivity* (Academic Press, New York–London, 1963).
32. C. Junge, Ann. Meteorol., Bd 5, 142–151 (1952).
33. M.V. Panchenko, A.G. Tumakov, and S.A. Terpugova, in: *Instrumentation for Remote Sensing of Atmospheric Parameters* (Tomsk Affiliate SB RAS, Tomsk, 1987), pp. 40–46.
34. V.V. Pol'kin and M.V. Panchenko, in: *Abstracts of Reports at V Workshop on Siberian Aerosols*, Tomsk (1998), pp. 91–93.
35. R. Leitch and W.J. Megaw, Indojaras **86**, Nos. 2–4, 217–225 (1981).